

	<b>SAKARYA ÜNİVERSİTESİ FEN BİLİMLERİ ENSTİTÜSÜ DERGİSİ</b> <i>SAKARYA UNIVERSITY JOURNAL OF SCIENCE</i>		
	<b>e-ISSN: 2147-835X</b> <b>Dergi sayfası: <a href="http://dergipark.gov.tr/saufenbilder">http://dergipark.gov.tr/saufenbilder</a></b>		
	<u>Geliş/Received</u> 07.03.2017 <u>Kabul/Accepted</u> 08.09.2017	<u>Doi</u> 10.16984/saufenbilder.296712	

## Numerical investigation of operating fluid, rotating disk speed effects and number of cavities on drag reduction of micro-textured surfaces for hydrodynamic lubrication

Ahmet Çağrı Develi\*<sup>1</sup>, Ali Bahadır Olcay<sup>2</sup>

### ABSTRACT

There have been developments on surface texturing methods providing benefit in a great many engineering applications. Especially, influence on surface texturing in lubrication applications related to frictional properties have been cause of concern. In the present study, it was aimed to work on the computational fluid dynamics (CFD) study of the lubrication system consisting of two parallel plates. While one of the plates was sliding, the other one was stationary and an incompressible two-dimensional single phase flow was assumed between those plates. The scope of the CFD analysis was to determine the relationship between drag force and operating fluid properties (i.e., oil types), rotational speed and the amount of the cavities. It was realized that SAE 0W-30 was found to be the best fluid among the seven studied oil types providing optimal conditions such as high drag reduction and less drag force. It was noticed that the drag coefficient thus, drag force appeared to be increasing as the rotating disk speed rose. The influence of the number of the cavities along the textured surface was also investigated in the present study and it was found that drag reduction was not associated with the number of cavities because 0, 1, 2 and 3 cavities nearly gave the same drag force values.

**Keywords:** Hydrodynamic lubrication; micro-textured surface; oil type; rotational speed; cavity; computational fluid dynamics (CFD)

### Hidrodinamik yağlamada kullanılan mikro-doku yüzeyler üzerinde akışkanın, diskin açısız hızının ve boşluk sayısının direnç azalmasına etkilerinin sayısal incelenmesi

### ÖZ

Yüzey dokusu yöntemlerinde gelişmeler yaşanırken bu gelişmelerden birçok mühendislik uygulamaları fayda sağlayabilir. Özellikle sürtünme özellikleri ile ilgili yağlama uygulamalarında yüzey dokusu etkisi önemli bir etkiye sahiptir. Bu çalışma kapsamında iki paralel plakadan oluşan yağlama sisteminin hesaplamalı akışkanlar dinamiği çalışmasıyla incelenmesi hedeflenmiştir. Plakalardan birisi hareket ederken, diğer plaka sabittir ve plakalar arasındaki akış, sıkıştırılmaz, iki boyutlu ve tek fazlı olarak kabul edildi. Hesaplamalı akışkanlar dinamiği analizinin amacı direnç kuvvetindeki azalmanın, çalışan akışkan özellikleri (yani yağ çeşidi), açısız hız ve boşluk miktarı ile nasıl ilişkili olduğunu belirlemektir. Bu çalışmada SAE 0W-30 tipi yağın, çalışılan yedi yağ arasında en yüksek direnç düşüşü ve daha az direnç kuvveti sağladığı için en uygun koşulları sağlayan akışkan olduğu belirlenmiştir. Direnç katsayısının ve dolayısıyla direnç kuvvetinin açısız hızın artmasıyla arttığı fark edilmiştir. Boşluk sayısının yüzey dokusuna etkisi de bu çalışma kapsamında araştırılmıştır ve dirençteki azalmanın boşluk sayısı ile ilişkili olmadığı bulunmuştur. Bunun nedeni 0, 1, 2 ve 3 boşluk yerleştirildiğinde neredeyse aynı direnç kuvvetleri elde edilmiştir.

**Anahtar Kelimeler:** Hidrodinamik yağlama; mikro-doku yüzeyi; yağ çeşidi; açısız hız; boşluk; hesaplamalı akışkanlar dinamiği (HAD)

\* Corresponding Author

<sup>1</sup> Faculty of Engineering, Mechanical Engineering Department, Yeditepe University, Turkey, ahmetcagrideveli@gmail.com

<sup>2</sup> Faculty of Engineering, Mechanical Engineering Department, Yeditepe University, Turkey, bahadir.olcay@yeditepe.edu.tr

## 1. INTRODUCTION

In recent years, there have been developments on surface texturing methods beneficial to many engineering applications. Especially, influence on surface texturing in lubrication applications related to frictional properties have been raised as an important concern by Hamilton et al. [1] and Anno et al. [2]. In their study, the impact of the cavity number, operating fluid and rotational speed on the hydrodynamic lubrication were evaluated. Their numerical model had two-dimensional parallel plates where one of them was sliding. There have been other experimental studies [3] conducted and succeeded marginal developments on hydrodynamic aspects in this field as well. For instance, Scaraggi et al. [4, 5] observed micro-cavity and depth effect of frictional characteristics experimentally. Moreover, a wide variety of numerical approaches have been proposed to estimate the properties of lubrication systems as regards the Reynolds or Navier-Stokes equations. In another study, Caramia et al. [6] approached the same phenomena both numerically and theoretically. They ran the same two-dimensional simulations in order to investigate the impact of the geometric parameters on the drag reduction and pressure forces. Specifically, they investigated the influence of cavity depth, height and gap on the drag reduction along with the pressure and viscous forces. They simulated a textured surface lubrication system, provided drag force calculation on the holder and defined a non-dimensional drag force. Furthermore, they focused the velocity profile in the micro-cavities and reported the results with effect of the shear stresses.

In hydrodynamic lubrication, the pressure condition of the fluid is crucial to assure better performance of the lubricated elements of components such as journal bearings. Therefore, experiments were proceeded to measure the pressure distribution around a journal bearing and frictional fluid force of the bearing caused by shearing reasons [7]. Kasolang et al. [7] utilized a journal diameter of 100 mm with variety of length-to-diameter ratio and obtained pressure results at different radial loads. They compared experimental results to estimated ones from established journal design charts (Raimondi and Boyd [8]). They also witnessed that the location

of the maximum pressure for the given operating conditions was almost same with the estimated value. Najjar et al. [9] solved Reynolds equation using finite difference method on the surface pad to determine pressure profile in the lubricant film. Their works assessed pressure at various locations. They showed that the maximum average value of pressure was roughly 12% larger than the former results. Von Gesseneck et al. [10] indicated a torque based method for remote displaying radially loaded deep groove ball bearings. They identified parameters of the bearing torque in time and frequency domains. Liming et al. [11] conducted thrust bearing lubrication analysis by combining finite element analysis with Reynolds equations. They used cyclic symmetric condition in order to simulate film flow. They found the influence of the rotational speed of the mirror plate on the lubrication characteristics indicated the thrust load had to be balanced against the oil film temperature and pressure for the optimized design perspectives. Susilowati et al. [12] investigated the hydrodynamic performance of journal bearing lubricated by thin film performed by three-dimensional computational fluid dynamics (CFD) model for two flow regimes as a main interest namely, laminar and turbulent regimes. They varied Reynolds number to see the significant effect on the hydrodynamic pressure. In a general view, their analysis concluded that characteristics of static hydrodynamic pressure indicate similar trends for laminar and turbulent regions.

In the present study, fluid flow characteristics of incompressible fluids between two parallel plates were numerically investigated to understand the lubrication behavior of the system. Mainly, the scope of the numerical analysis was to determine effect of rotational speeds, operating fluid properties and cavities on drag force reduction. The current study had a numerical model similar to Caramia et al. [6]; therefore, the numerical model was first validated based on non-dimensional drag force findings of that work. Then, authors reported their validation in terms of the test results by Scaraggi et al. [4, 5]. Following that, mesh convergence tests were performed by monitoring the velocity profile at the gap, drag coefficient and non-dimensional drag force. Once the validated numerical model was obtained, dependency of drag force reduction on rotational speed, operating fluid conditions and cavity numbers were reported in the present investigation. Finally, computational domains

with and without cavities were also studied by evaluating reduction in drag force of the system.

## 2. NUMERICAL DOMAIN

Caramia et al. [6] inspired from the pin-on-disk tribometer experimental set up of Scaraggi et al. [4, 5] for friction measurements. Scaraggi et al. [4, 5] conducted experimental tests with different laser-textured bearing balls joined together in the pin holder as shown in Figure 1. Caramia et al. [6] specifically focused on the surface between ball holder and disk holder. Therefore, they utilized a two-dimensional computational model along with boundary conditions as shown in Figure 2 to provide a theoretical explanation by using numerical approach. The detail dimensioning (enlarged view of dashed rectangle in Figure 2) of textured surface with the geometric parameters computational model are illustrated in Figure 3 and the related parameters are provided in Table 1. They presented nearly 80% drag reduction for different dimensions and flow rates [6].

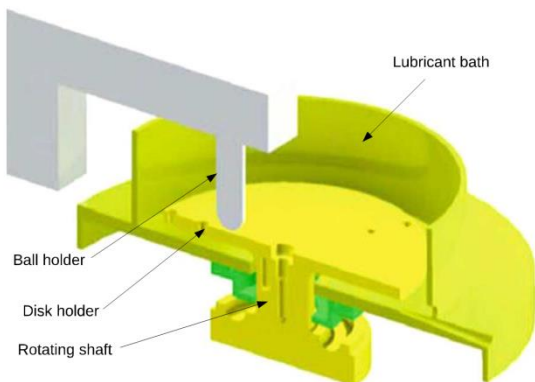


Figure 1. Experimental setup sketch by Scaraggi et al. [4, 5]

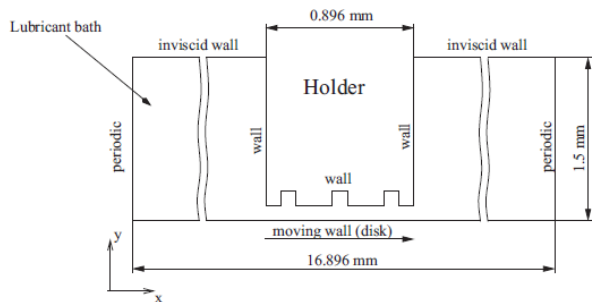


Figure 2. Computational geometry and boundary conditions by Caramia et al. [6]

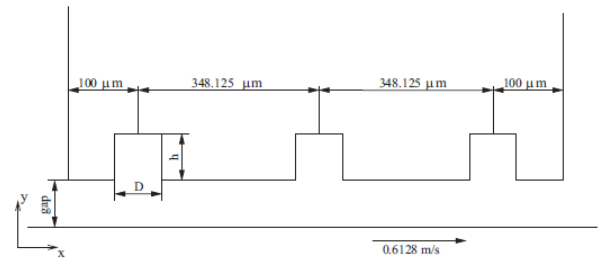


Figure 3. Local view of the textured surface with the geometric parameters displayed

Table 1. Dimensions of the geometric parameters of Caramia et al. [6]

Parameter	Size
D (μm)	25
h (μm)	1
gap (μm)	1

In the present study, a two-dimensional computational model identical with Caramia et al. [6] was generated. Left and right vertical boundaries were very far from the holder; therefore, these boundaries were assigned as periodic boundaries to isolate the pin holder. At lower band of the geometry, the moving wall boundary condition was applied to represent the rotating disk. The flat wall movement was defined with a velocity of 0.6128 m/s in Caramia et al.'s [6] study; but, this velocity was varied to understand the effect of velocity on the drag coefficient in the present study. Inviscid boundary condition was defined for the upper side and this ensured slip condition meaning that no frictional forces were considered. However, pin holder was crucial for the simulation and assumed as no slip condition. The wall of the pin holder and moving wall was also modeled in more detail due to importance for the result of the drag force reduction. Quadrilateral elements were employed for the whole domain instead of triangular elements which was used by Caramia et al. [6]. Particularly, more elements compared to the other part of the domain were placed at the corner of the cavities to capture velocity gradients in that region accurately as seen in Figure 4.

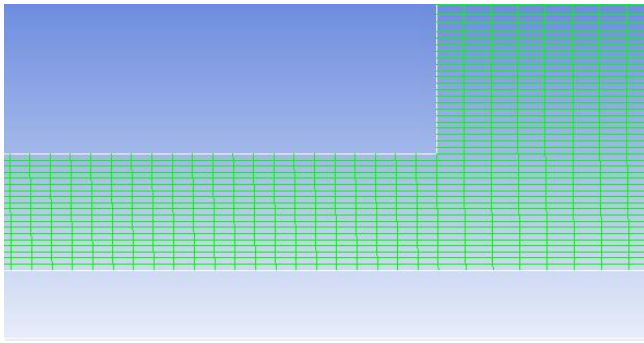


Figure 4. Quadrilateral elements at the corner of the cavity

The minimum grid dimension was specified as  $0.25 \mu\text{m}$  near the wall and mesh independency study was also performed to validate the results with findings of earlier work. Variations of non-dimensional drag force, drag coefficient defined as the ratio of the actual flow rate to theoretical flow rate and the velocity profile at the center of the cavity with respect to total grid number were monitored to check whether the results were grid dependent or not. Velocity profile at the center cavity was also evaluated and plotted in Figure 5. It was noted that use of 2 million elements in CFD model helped to capture the characteristics of velocity profile at the center cavity better than the use of 1.2 million and 0.6 million as shown in Figure 5. Those results by Caramia et al. [6] were also discussed to support the validation of the mesh independency study in the same plot. Briefly, the results showed that  $C_d = 45.19$  for the cells with a number of 2 million,  $C_d = 45.94$  for the cells with a number of 1.2 million and  $C_d = 44.27$  for 0.6 million as provided in Table 2. As to compare the non-dimensional drag force, the value of 944 for 2 million elements, 942.81 for 1.2 million elements and 925.04 for 0.6 million elements as given in Table 2. Caramia et al. [6] divided the micro channel in 20 at y axis and reported that value of the non-dimensional drag force is around about 943. We proceed to the studies in this article with CFD model having 2000000 elements and obtained non-dimensional drag force to be 944 within 0.1% difference from Caramia et al.'s [6] finding.

Table 2. Drag coefficient and non-dimensional drag force comparison with Caramia et al. [6]

Number of elements	$C_d$	$T$
600000 elements	44.27	925.04
1200000 elements	45.12	942.81
2000000 elements	45.19	944
Caramia et al. (1200000 elements)	45.14	943.15

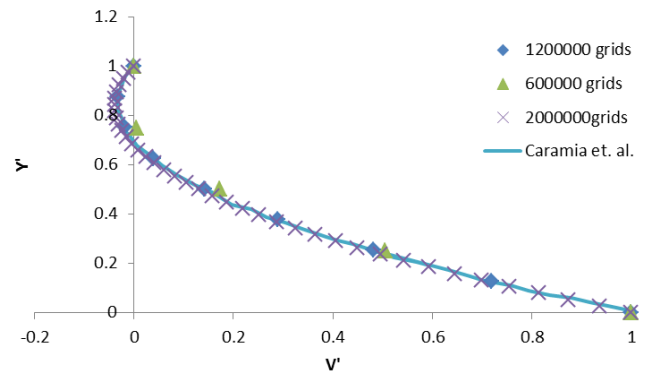


Figure 5. Velocity profile at the center cavity

Fluid flow characteristics in the gap between parallel plates were simulated using computational fluid dynamics (CFD) software, namely Ansys Fluent 12. The governing equations, namely continuity and two-dimensional Navier-Stokes equations given in equations (1) and (2), were solved using a finite volume method for laminar incompressible fluid flow to determine the velocity field and drag coefficients. The solver scheme was selected to be second order accurate and the SIMPLE algorithm was utilized for pressure-velocity coupling while second order upwind scheme was used in discretization of convective terms. Lastly, the convergence criteria were set to  $10^{-4}$  for simulations.

$$(\bar{u} \cdot \nabla) \bar{u} = -\nabla p + \frac{1}{Re} \nabla^2 \bar{u} \quad (1)$$

$$\nabla \bar{u} = 0 \quad (2)$$

Here,  $p$  was pressure,  $\bar{u}$  was the velocity vector and  $Re$  was the Reynolds number and defined as;

$$Re = \frac{\rho U gap}{\mu} \quad (3)$$

where  $\rho$  was the fluid density,  $\mu$  the dynamic viscosity of the operating fluid,  $U$  was the rotating disk (moving wall) velocity and gap was the distance between plates and set to  $1 \mu\text{m}$  for CFD model. The non-dimensional drag force was defined by Caramia et al. [6] as below;

$$T = \frac{F_x}{\mu UL} \quad (4)$$

where  $L$  was the unitary length and  $F_x$  was the drag force calculated as  $F_x = C_d A_{wet} \frac{1}{2} \rho U^2$ . Here,  $A_{wet}$  represented the surface area of the pin holder and  $C_d$  was the drag coefficient.

### 3. RESULTS AND DISCUSSION

#### 3.1. Effect of Operating Fluid in Lubrication Flow

In the present study, we have selected seven oil types with different in densities and dynamic viscosities to understand what type of fluid works with lowest drag. It was observed that drag coefficient; thus, drag force depended on the viscosity of the fluid. Table 3 shows viscosity and density values of different oil types used in this study. These fluids were used as working fluids in CFD simulations to determine the optimum oil providing the most reduction in drag. Figure 6 displays the reduction in drag force in terms of oil types. As one can remember, Reynolds number was calculated based on rotating disk velocity in order to discuss effect of the fluid type over the reduction in drag force in this study. Therefore, moving wall speed was maintained constant at 0.6128 m/s for all simulations for each operating oils. As it appears, SAE 0W-30 oil provided minimum drag force and was the best of all along the other studied fluids given in Table 3. However, both SAE 50 and SAE 10W-60 oils have higher kinematic viscosities than other oils tabulated in Table 3. For example, SAE 15W-40 oil may seem to be the optimum liquid for the lubrication system to provide high reduction in drag force because of drag coefficient and influence of the dynamic viscosity on the drag force. Noting that the velocity of the rotating disk and gap between the parallel plates were same for all evaluations and drag coefficient was directly proportional to the kinematic viscosity and inversely proportional to Reynolds number. As per Figure 7, the drag force increases as the kinematic viscosity increases. This is probably due to fact that viscous fluids cause high drags because of frictional losses. Furthermore, as the molecular motions in the fluid are getting more restricted, drag force against fluid flow increases exponentially. Therefore, the reduction in drag force or the non-dimensional drag force is optimal at a certain range of Reynolds number.

Table 3. Density and dynamic viscosity of operating fluids [13]

Type of oil	Density (kg/m <sup>3</sup> )	Dynamic viscosity (Pa.s)
SAE 15W-40	866.3	0.091057
SAE 10W-40	850.5	0.07933
SAE 10W-60	838	0.13552
SAE 5W-40	842.1	0.076651
SAE 0W-30	837.2	0.055926
SAE 30	869.3	0.07455
SAE 50	900	0.2403

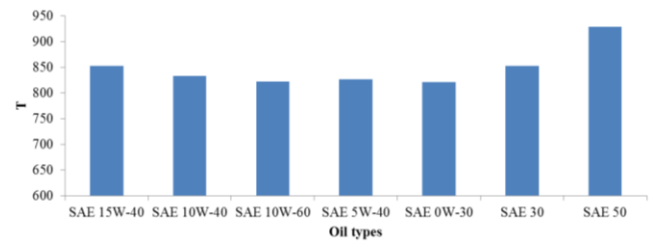


Figure 6. Reduction in non-dimensional drag force versus type of oils for moving wall speed at 0.6128 m/s

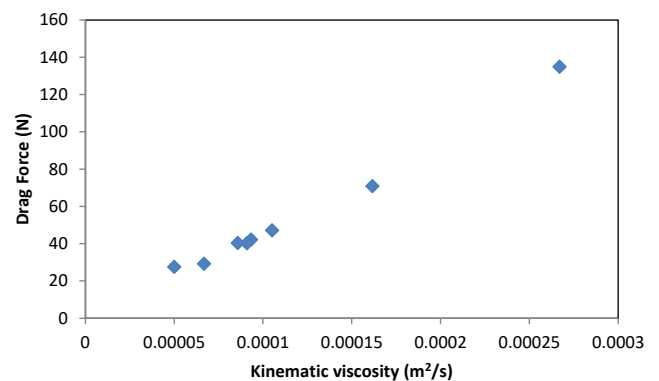


Figure 7. Drag force with respect to kinematic viscosity

#### 3.2. Effect of Reynolds Number in Lubrication Flow of the Pin Holder

In the present study, drag coefficient, reduction in drag force and drag force variation with Reynolds number were investigated. Figure 8 shows the change of drag coefficient along with Reynolds number. It was noted drag coefficient exhibited sharp decrease when Reynolds number was varied from 0.002 to 0.008. Then, drag coefficient stayed around 45. This indicated that Reynolds number needed to be larger than 0.007 so that smaller drag coefficients could be achieved.

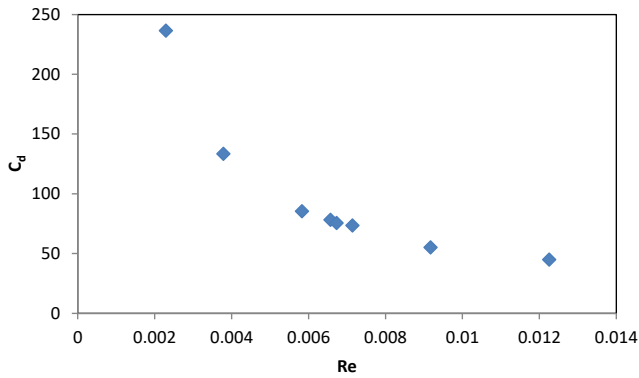


Figure 8. Drag coefficient with respect to Reynolds number

It was known that drag force typically increases significantly as the fluid velocity increases for very low Reynolds numbers ( $Re \ll 1$ ). Due to increase in drag force, non-dimensional drag force was elevated as Reynolds number increased as seen in Figure 9. For this analysis, SAE 0W-30 was selected as an operating fluid and increase in non-dimensional drag force was observed when Reynolds number was raised in Figure 9.

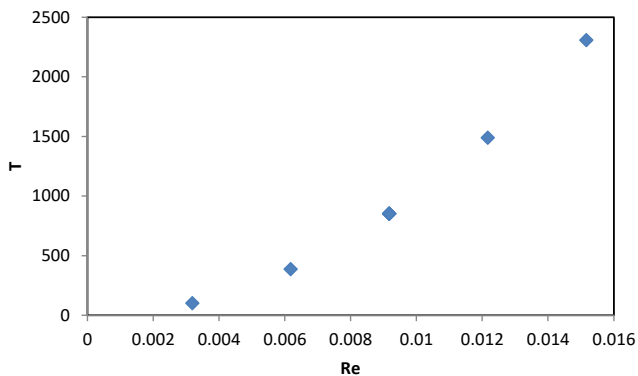


Figure 9. Reduction in drag force trend over Reynolds number

Variation of drag force was also obtained by varying wall velocity from 0.2 to 1 m/s and plotted in Figure 10. It was realized that increase in wall velocity caused increase in Reynolds number; therefore, resulting drag force appeared to be rising when the rotating disk speed was increased.

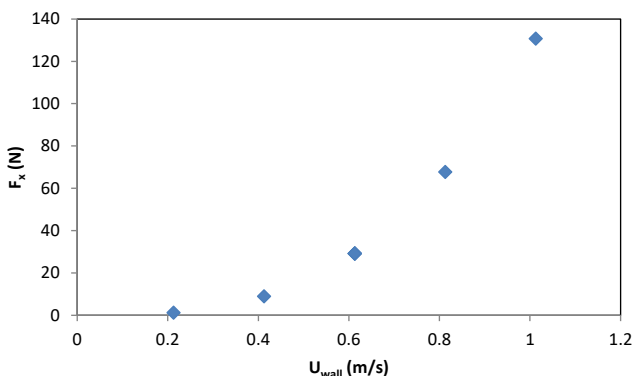


Figure 10. Drag force increasing with rotating disk velocity

### 3.3. Effect of Number of Cavities on Reduction in Force

In the present study, the effect of number of the cavities in CFD model was also investigated to determine whether the drag force can be affected or not with more or less cavities. Therefore, we based our results by choosing no cavity along the texture surface as the starting point. Then, cavities were added to the each simulation to determine drag force. Figure 11 and 12 show drag force and reduction in drag force with respect to number of cavities, respectively. It was noted that number of cavities did not have any significant effect on either drag force or drag reduction. Therefore, drag stayed nearly the same when number of cavities was changed from 0 to 1, 1 to 2 and 2 to 3. This implied that no reduction in drag force can be achieved with more or less number of cavities for the studied cases.

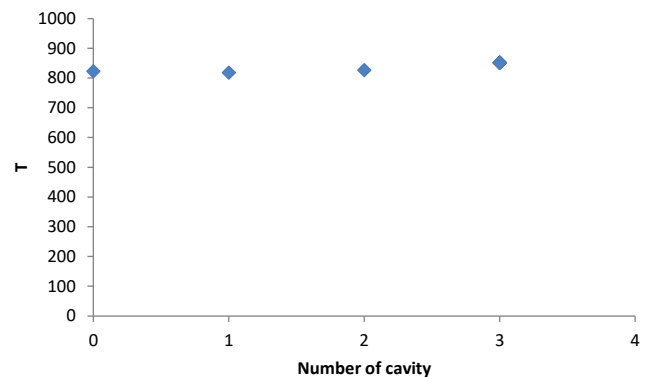


Figure 11. The drag force due to number of cavity

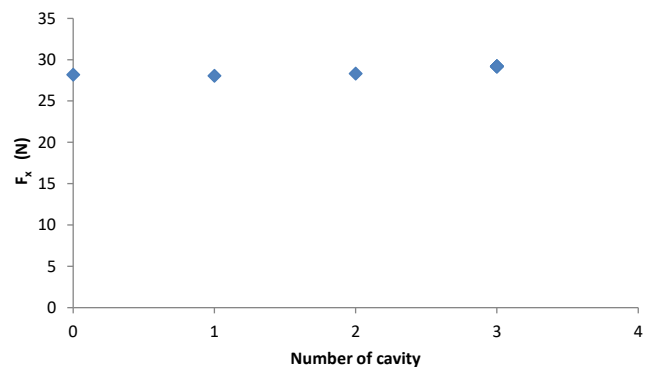


Figure 12. Reduction in drag force due to number of cavity

## 4. CONCLUSION

The hydrodynamic lubrication system which consists of parallel micro-textured surfaces was analyzed for incompressible two-dimensional flows and the generated numerical model was

validated by using flow velocity profile given by Caramia et al. [6]. Seven different types of oils were used as operating fluids and CFD simulations were performed to determine the oil with optimal conditions. It was noted that SAE 0W-30 was found to be the best fluid providing optimal conditions such as high reduction in drag force and less drag force. Moreover, the rotating disk speed was varied to produce different conditions to simulate the flow along the textured surface. The drag force and reduction in drag force were observed for each rotating disk velocity conditions. It was realized that the drag coefficient thus, drag force appeared to be increasing as the rotating disk speed rose. Specifically, when wall velocity was increased from 0.2 m/s to 1 m/s, corresponding drag force was drastically raised from nearly zero to over 130 N. This implies that rotational speed has a key role in drag force determination. The influence of the number of the cavities along the textured surface was also investigated in the present study and it was found that reduction in drag force was not associated with the number of cavities because 0, 1, 2 and 3 cavities nearly gave the same drag force values.

## REFERENCES

- [1] D. Hamilton, J. Walowit, and C. Allen, "A theory of lubrication by microirregularities," *Journal of Basic Engineering*, vol. 88, pp. 177-185, 1966.
- [2] J. N. Anno, J. Walowit, and C. Allen, "Microasperity lubrication," *Journal of Lubrication Technology*, vol. 90, pp. 351-355, 1968.
- [3] V. G. Marian, D. Gabriel, G. Knoll, and S. Filippone, "Theoretical and experimental analysis of a laser textured thrust bearing," *Tribology letters*, vol. 44, p. 335, 2011.
- [4] M. Scaraggi, F. P. Mezzapesa, G. Carbone, A. Ancona, D. Sorgente, and P. M. Lugarà, "Minimize friction of lubricated laser-microtextured-surfaces by tuning microholes depth," *Tribology International*, vol. 75, pp. 123-127, 2014.
- [5] M. Scaraggi, F. P. Mezzapesa, G. Carbone, A. Ancona, and L. Tricarico, "Friction properties of lubricated laser-microtextured-surfaces: an experimental study from boundary-to hydrodynamic-lubrication," *Tribology Letters*, vol. 49, pp. 117-125, 2013.
- [6] G. Caramia, G. Carbone, and P. De Palma, "Hydrodynamic lubrication of micro-textured surfaces: two dimensional CFD-analysis," *Tribology International*, vol. 88, pp. 162-169, 2015.
- [7] S. Kasolang, M. A. Ahmad, R.-D. Joyce, and C. F. M. Tai, "Preliminary study of pressure profile in hydrodynamic lubrication journal bearing," *Procedia Engineering*, vol. 41, pp. 1743-1749, 2012.
- [8] A. Raimondi and J. Boyd, "A solution for the finite journal bearing and its application to analysis and design: II," *ASLE Transactions*, vol. 1, pp. 175-193, 1958.
- [9] F. A. Najjar and G. Harmain, "Numerical Investigation of Pressure Profile in Hydrodynamic Lubrication Thrust Bearing," *International scholarly research notices*, vol. 2014, 2014.
- [10] J. J. von Gesseneck, B. Caers, M. Van Overmeire, D. Lefeber, B. Vanderborght, and P. Schuurmans, "A torque-based method for the study of roller bearing degradation under poor lubrication conditions in a lead-bismuth environment," *Nuclear Engineering and Design*, vol. 305, pp. 121-131, 2016.
- [11] L. Zhai, Y. Luo, Z. Wang, and X. Liu, "3D Two-way coupled TEHD analysis on the lubricating characteristics of thrust bearings in pump-turbine units by combining CFD and FEA," *Chinese Journal of Mechanical Engineering*, vol. 29, pp. 112-123, 2016.
- [12] M. Tauviquirrahman, J. Jamari, and A. P. Bayuseno, "A Comparative Study of Finite Journal Bearing in Laminar and Turbulent Regimes Using CFD (Computational Fluid Dynamic)," in *MATEC Web of Conferences*, 2016.
- [13] Available: <http://www.viscopedia.com/viscosity-tables/substances/engine-oil/>. [Accessed: 29-May-2016].